Stochastic Integration Filter: Theoretical and Implementation Aspects

Jindřich Havlík
Department of Cybernetics
University of West Bohemia
Plzen, Czech Republic
havlikj@ntis.zcu.cz

Ondřej Straka
Department of Cybernetics
University of West Bohemia
Plzen, Czech Republic
straka30@kky.zcu.cz

Uwe D. Hanebeck
Institute for Anthropomatics and Robotics
Karlsruhe Institute of Technology
Karlsruhe, Germany
uwe.hanebeck@ieee.org

***Abstract*— The paper focuses on state estimation of discrete-time nonlinear stochastic dynamic systems with a special focus on the stochastic integration filter. The filter is an representative of the Gaussian filter and computes the state and measurement predictive moments by making use of a stochastic integration rule. As a result, the calculated values of the moments are random variables and exhibit favorable asymptotic properties. The paper analyzes theoretical consequences of using stochastic integration rules and proposes several modifications that improve the performance of the stochastic integration filter. As the filter requires multiple iterations of the stochastic rule, its computational costs are higher in comparison with other Gaussian filters. To reduce the costs, several modifications are proposed in the paper, which are also concerned with numerical stability issues. The proposed modifications are illustrated using both static and dynamic numerical examples used in target tracking.**

***Index Terms*—state estimation, Gaussian filter, stochastic integration rule**

I. Introduction

Nonlinear state estimation of discrete-time stochastic dynamic systems is a broad field of study, which has attracted significant attention in the last decades. It plays a crucial role in many areas such as signal processing [1], target tracking [2], satellite navigation [3], fault detection and isolation [4], and optimal and predictive control problems [5]. The state estimation problem is generally solved by the Bayesian recursive relations (BRRs) [6]. They provide the state estimate in the form of a conditional probability density function (PDF) of the state conditioned by the measurement. The conditional PDF provides full information about the unknown state. Due to intractability of the BRRs for nonlinear or non-Gaussian systems, the closed form solution to the problem often relies on appropriate approximations.

Methods providing approximate conditional PDFs capturing the complexity of the conditional PDF with high fidelity are called global methods. They are represented, e.g., by the Gaussian sum method [7], the point-mass method [8], and the particle filter [9]. Their practical use is limited especially due to their excessive computational complexity.

By assuming a Gaussian joint PDF of the state and measurement, the BRRs lead to the methods known as Gaussian filters (GFs) [10] or local Bayesian methods [11]. The GFs possess the same structure of the algorithm, where the particular GF is given by the approximations used for evaluating integrals involved in state and measurement moments computation constituting the GF algorithm core. The GFs are represented namely by the quadrature Kalman filter [12] employing a quadrature rule, the cubature Kalman filter [11] employing a cubature rule, the cubature quadrature Kalman filter [13], the sparse-grid quadrature filter [14], the smart sampling Kalman filter [15], or the stochastic integration filter (SIF) [16], which utilizes a stochastic integration rule (SIR) [17].

The SIR is based on an iterative evaluation of randomized spherical and radial rules. As a consequence, the SIR estimates the integral values by random quantities instead of deterministic quantities and has an advantage compared to the other numerical rules as it provides an integral value error estimate. The original SIF algorithm proposed in [16] merely combines the GF algorithm and the SIR. However, a detailed analysis of implications of using random quantities approximating integral values is not available. Also, nice asymptotic properties of the random integral evaluations hold for a large number of iterations, which may be infeasible in many SIF applications.

The goal of the paper is twofold. First, the paper focuses on theoretical aspects of using random integral values in the algorithm of the GF. Second, the paper treats implementation aspects with a focus to lowering computational demands while maintaining numerical stability of the SIF.

The rest of the paper is organized as follows: Section 2 is devoted to a brief introduction to the nonlinear state estimation and its solution by the GFs, especially the SIF. Section 3 reveals the consequences of random integral values occurring in the algorithm of the GF. Section 4 proposes possible modifications of the SIF algorithm in order to deliver results with lower computational demands. In Section 5, comprehensive numerical illustrations are used to picture the properties of the proposed theoretical and implementation modifications and the paper is concluded by Section 6.

II. Problem Formulation and Stochastic Integration Filter

This section formulates the nonlinear state estimation problem, presents its GF solution, and describes the SIF.

The work was supported by the Czech Ministry of Education, Youth and Sports, project LO1506 and by the Czech Science Foundation, project no. GA 16-19999J.

A. Formulation of the Nonlinear State Estimation Problem

Let a discrete-time nonlinear stochastic dynamic model be considered in the following state-space form

$$\mathbf{x}_{k+1} = \mathbf{f}_k(\mathbf{x}_k) + \mathbf{w}_k, \quad k = 0, 1, 2, \ldots, \tag{1}$$

$$\mathbf{z}_k = \mathbf{h}_k(\mathbf{x}_k) + \mathbf{v}_k, \quad k = 0, 1, 2, \ldots, \tag{2}$$

where the vectors $\mathbf{x}_k \in \mathbb{R}^{n_x}$ and $\mathbf{z}_k \in \mathbb{R}^{n_z}$ represent the state and the measurement at time instant k, respectively, $\mathbf{f}_k : \mathbb{R}^{n_x} \to \mathbb{R}^{n_x}$ and $\mathbf{h}_k : \mathbb{R}^{n_x} \to \mathbb{R}^{n_z}$ are known vector functions, and $\mathbf{w}_k \in \mathbb{R}^{n_x}$ and $\mathbf{v}_k \in \mathbb{R}^{n_z}$ are mutually independent state and measurement white noises. The PDFs[1] of the noises are Gaussian with zero means and known covariance matrices[2] (CMs) $\mathbf{\Sigma}_k^{\mathbf{w}}$ and $\mathbf{\Sigma}_k^{\mathbf{v}}$, respectively, i.e., $p(\mathbf{w}_k) = \mathcal{N}\{\mathbf{w}_k; \mathbf{0}_{n_x \times 1}, \mathbf{\Sigma}_k^{\mathbf{w}}\}$ and $p(\mathbf{v}_k) = \mathcal{N}\{\mathbf{v}_k; \mathbf{0}_{n_z \times 1}, \mathbf{\Sigma}_k^{\mathbf{v}}\}$, where $\mathbf{0}_{a \times b}$ denotes an $a \times b$ matrix of zeros. The PDF of the initial state is Gaussian and known as well, i.e., $p(\mathbf{x}_0) = \mathcal{N}\{\mathbf{x}_0; \hat{\mathbf{x}}_0, \mathbf{P}_0\}$. The initial state is independent of the noises.

The state estimation aims at searching for the state $\mathbf{x}_k$ based on the measurements up to the time instant ℓ, which will be denoted as $\mathbf{z}^\ell \triangleq [\mathbf{z}_0^T, \mathbf{z}_1^T, \ldots, \mathbf{z}_\ell^T]^T$. Due to the stochastic nature of the system, the state estimate is described by the conditional PDF $p(\mathbf{x}_k|\mathbf{z}^\ell)$. In this paper, the filtering ($\ell = k$) and the one-step prediction ($\ell = k-1$) problems will be considered only. To find the filtering estimate $p(\mathbf{x}_k|\mathbf{z}^k)$, the Bayesian approach uses the following BRRs providing the solution [6]

$$p(\mathbf{x}_k|\mathbf{z}^k) = \frac{p(\mathbf{x}_k|\mathbf{z}^{k-1}) p(\mathbf{z}_k|\mathbf{x}_k)}{\int p(\mathbf{x}_k|\mathbf{z}^{k-1}) p(\mathbf{z}_k|\mathbf{x}_k)\, \mathrm{d}\mathbf{x}_k}, \tag{3}$$

where the one-step prediction PDF is

$$p(\mathbf{x}_k|\mathbf{z}^{k-1}) = \int p(\mathbf{x}_{k-1}|\mathbf{z}^{k-1}) p(\mathbf{x}_k|\mathbf{x}_{k-1})\, \mathrm{d}\mathbf{x}_{k-1}, \tag{4}$$

with $p(\mathbf{x}_k|\mathbf{x}_{k-1}) = p_{\mathbf{w}_{k-1}}(\mathbf{x}_k - \mathbf{f}_{k-1}(\mathbf{x}_{k-1}))$ and $p(\mathbf{z}_k|\mathbf{x}_k) = p_{\mathbf{v}_k}(\mathbf{z}_k - \mathbf{h}_k(\mathbf{x}_k))$.

An analytic solution to (3) and (4) is an intricate functional-domain problem, which can be computed for a few special cases only. Such a case is, for example, given by linear functions $\mathbf{f}_k$ and $\mathbf{h}_k$ in the model equations (1) and (2). For a nonlinear system approximate solutions are typically sought.

Principal approximations are of two types. The first type of approximations involves numerical solutions to the BRRs. The point-mass method [8] or the particle filter [9] are significant representatives of the numerical approximate methods.

The second type of approximations is based on an analytic solution. This can be achieved by more restrictive approximations or assumptions. For example, by approximating the PDFs by a Gaussian mixture PDF, the Gaussian sum method [7] is obtained. The Gaussian mixture representation maintains a global validity of the results. However, simpler methods, assuming Gaussian PDFs are more popular. Such filters are denoted as Gaussian filters [10].

[1]For the sake of simplicity all PDFs will be given by their argument, if not stated otherwise, i.e., $p(\mathbf{w}_k) = p_{\mathbf{w}_k}(\mathbf{w}_k)$.

[2]Through the paper, symbols $\mathbb{E}, \mathbb{V}, \mathbb{C}$ are used for mean, variance and cross-covariance, respectively, i.e., $\mathbb{C}[\mathbf{x}, \mathbf{y}] = \mathbb{E}[(\mathbf{x} - \mathbb{E}[\mathbf{x}])(\mathbf{y} - \mathbb{E}[\mathbf{y}])^T]$, $\mathbb{V}[\mathbf{x}] = \mathbb{C}[\mathbf{x}, \mathbf{x}]$, whereas the term CM can mean both variance and cross-covariance.

B. Gaussian Filters

In addition to assuming Gaussianity of states and measurements, the GFs also assume the joint predictive PDF $p(\mathbf{z}_k, \mathbf{x}_k|\mathbf{z}^{k-1})$ being Gaussian at each time instant [11]

$$p(\mathbf{z}_k, \mathbf{x}_k|\mathbf{z}^{k-1}) = \mathcal{N}\left\{ \begin{bmatrix} \mathbf{z}_k \\ \mathbf{x}_k \end{bmatrix}; \begin{bmatrix} \hat{\mathbf{z}}_{k|k-1} \\ \hat{\mathbf{x}}_{k|k-1} \end{bmatrix}, \begin{bmatrix} \mathbf{P}^{\mathbf{zz}}_{k|k-1} & \mathbf{P}^{\mathbf{xz}\,T}_{k|k-1} \\ \mathbf{P}^{\mathbf{xz}}_{k|k-1} & \mathbf{P}^{\mathbf{xx}}_{k|k-1} \end{bmatrix} \right\}. \tag{5}$$

By adopting these Gaussian assumptions, the filtering PDF $p(\mathbf{x}_k|\mathbf{z}^k)$ and the one-step predictive PDF $p(\mathbf{x}_k|\mathbf{z}^{k-1})$ are also Gaussian

$$p(\mathbf{x}_k|\mathbf{z}^k) = \mathcal{N}\{\mathbf{x}_k; \hat{\mathbf{x}}_{k|k}, \mathbf{P}^{\mathbf{xx}}_{k|k}\}, \tag{6}$$

$$p(\mathbf{x}_k|\mathbf{z}^{k-1}) = \mathcal{N}\{\mathbf{x}_k; \hat{\mathbf{x}}_{k|k-1}, \mathbf{P}^{\mathbf{xx}}_{k|k-1}\}. \tag{7}$$

Since only Gaussian distributions (5) are considered, calculation of the first two moments of (5) is sufficient.

The algorithm of the GF is described in the **Algorithm 1**.

Algorithm 1: Gaussian Filter

Step 1: (*initialization*) Set the time step $k = 0$ and define a priori initial condition by its first two moments

$$\hat{\mathbf{x}}_{0|-1} \triangleq \mathbb{E}[\mathbf{x}_0] = \hat{\mathbf{x}}_0, \tag{8}$$

$$\mathbf{P}^{\mathbf{xx}}_{0|-1} \triangleq \mathbb{V}[\mathbf{x}_0] = \mathbf{P}_0. \tag{9}$$

Step 2: (*filtering, measurement update*) The filtering mean $\hat{\mathbf{x}}_{k|k}$ and CM $\mathbf{P}^{\mathbf{xx}}_{k|k}$ are computed by means of

$$\hat{\mathbf{x}}_{k|k} = \hat{\mathbf{x}}_{k|k-1} + \mathbf{K}_k(\mathbf{z}_k - \hat{\mathbf{z}}_{k|k-1}), \tag{10}$$

$$\mathbf{P}^{\mathbf{xx}}_{k|k} = \mathbf{P}^{\mathbf{xx}}_{k|k-1} - \mathbf{K}_k \mathbf{P}^{\mathbf{zz}}_{k|k-1} \mathbf{K}_k^T, \tag{11}$$

where

$$\mathbf{K}_k = \mathbf{P}^{\mathbf{xz}}_{k|k-1} (\mathbf{P}^{\mathbf{zz}}_{k|k-1})^{-1} \tag{12}$$

is the filter gain and the measurement prediction $\hat{\mathbf{z}}_{k|k-1}$ is given by

$$\hat{\mathbf{z}}_{k|k-1} = \mathbb{E}[\mathbf{z}_k|\mathbf{z}^{k-1}] = \mathbb{E}\big[\mathbf{h}_k(\mathbf{x}_k)|\mathbf{z}^{k-1}\big]. \tag{13}$$

The predictive CMs $\mathbf{P}^{\mathbf{xz}}_{k|k-1}$ and $\mathbf{P}^{\mathbf{zz}}_{k|k-1}$ are computed as

$$\begin{aligned} \mathbf{P}^{\mathbf{zz}}_{k|k-1} &= \mathbb{E}[(\mathbf{z}_k - \hat{\mathbf{z}}_{k|k-1})(\mathbf{z}_k - \hat{\mathbf{z}}_{k|k-1})^T|\mathbf{z}^{k-1}] \\ &= \mathbb{E}[(\mathbf{h}_k(\mathbf{x}_k) - \hat{\mathbf{z}}_{k|k-1})(\cdot)^T|\mathbf{z}^{k-1}] + \mathbf{\Sigma}_k^{\mathbf{v}} \\ &= \mathbb{V}\big[\mathbf{h}_k(\mathbf{x}_k)|\mathbf{z}^{k-1}\big] + \mathbf{\Sigma}_k^{\mathbf{v}}, \end{aligned} \tag{14}$$

$$\begin{aligned} \mathbf{P}^{\mathbf{xz}}_{k|k-1} &= \mathbb{E}[(\mathbf{x}_k - \hat{\mathbf{x}}_{k|k-1})(\mathbf{z}_k - \hat{\mathbf{z}}_{k|k-1})^T|\mathbf{z}^{k-1}] \\ &= \mathbb{E}[(\mathbf{x}_k - \hat{\mathbf{x}}_{k|k-1})(\mathbf{h}_k(\mathbf{x}_k) - \hat{\mathbf{z}}_{k|k-1})^T|\mathbf{z}^{k-1}] \\ &= \mathbb{C}\big[\mathbf{x}_k, \mathbf{h}_k(\mathbf{x}_k)|\mathbf{z}^{k-1}\big]. \end{aligned} \tag{15}$$

Step 3: (*prediction, time update*) The predictive mean $\hat{\mathbf{x}}_{k+1|k}$ and CM $\mathbf{P}^{\mathbf{xx}}_{k+1|k}$ are given by

$$\hat{\mathbf{x}}_{k+1|k} = \mathbb{E}[\mathbf{x}_{k+1}|\mathbf{z}^k] = \mathbb{E}[\mathbf{f}_k(\mathbf{x}_k)|\mathbf{z}^k], \tag{16}$$

$$\begin{aligned} \mathbf{P}^{\mathbf{xx}}_{k+1|k} &= \mathbb{E}[(\mathbf{x}_{k+1} - \hat{\mathbf{x}}_{k+1|k})(\mathbf{x}_{k+1} - \hat{\mathbf{x}}_{k+1|k})^T|\mathbf{z}^k] \\ &= \mathbb{E}[(\mathbf{f}_k(\mathbf{x}_k) - \hat{\mathbf{x}}_{k+1|k})(\cdot)^T|\mathbf{z}^k] + \mathbf{\Sigma}_k^{\mathbf{w}} \\ &= \mathbb{V}\big[\mathbf{f}_k(\mathbf{x}_k)|\mathbf{z}^k\big] + \mathbf{\Sigma}_k^{\mathbf{w}}. \end{aligned} \tag{17}$$

Let $k = k + 1$. The algorithm then continues by **Step 2**.

The moments (13) – (17) can be expressed in the following general form of Gaussian weighted integral

$$\mathbf{I}_{\boldsymbol{\gamma}} \triangleq \mathbb{E}[\boldsymbol{\gamma}(\mathbf{x})] = \int \boldsymbol{\gamma}(\mathbf{x})\, \mathcal{N}\{\mathbf{x}; \mathbf{m}, \mathbf{P}\}\, \mathrm{d}\mathbf{x}\,, \tag{18}$$

where $\boldsymbol{\gamma} : \mathbb{R}^{n_x} \rightarrow \mathbb{R}^{n_\gamma}$ is a vector function (for example $\mathbf{f}_k(\mathbf{x})$), $\mathbf{m} = \mathbb{E}[\mathbf{x}]$ is the mean, and $\mathbf{P} = \mathbb{V}[\mathbf{x}]$ is the CM of $\mathbf{x} \in \mathbb{R}^{n_x}$.

The particular GFs vary in the way they evaluate the Gaussian PDF weighted integral (18). The GFs employ deterministic or stochastic numerical integration rules.

The rules approximate the integral by a sum of weighted points[3] transformed through $\boldsymbol{\gamma}$. The points and corresponding weights are specifically selected such that the approximate sum is exact for polynomial functions $\boldsymbol{\gamma}(\mathbf{x})$ up to a certain degree. The particular filters are known as the quadrature Kalman filter [12], the cubature Kalman filter [11], the cubature quadrature Kalman filter [13], the sparse-grid quadrature filter [14], or the SIF [16], or the smart sampling Kalman filter [15], which is approximate and derived via distance measures.

C. Stochastic Integration Filter

The SIF [16] employs the SIR [17] for evaluating integrals of the form (18) arising in the algorithm of the GF. The main advantage of the SIR is that it guarantees asymptotically exact evaluation of the integrals.

The **Algorithm 2** illustrates the degree 3 SIR, which is exact for degree 3 polynomials, for computing an approximate value of $\mathbf{I}_{\boldsymbol{\gamma}}$ in (18).

Algorithm 2 Degree 3 Stochastic Integration Rule

Step 1: Select a maximum number of iterations N or an error tolerance ε.

Step 2: Set the current iteration number $i = 0$, initial value of the integral $\bar{\mathbf{I}}^0_{\boldsymbol{\gamma}} = \mathbf{0}_{n_\gamma \times 1}$ and initial square error of the integral $\bar{\mathbf{V}}^0_{\boldsymbol{\gamma}} = \mathbf{0}_{n_\gamma \times n_\gamma}$.

Step 3: Repeat (until $i = N$ or $||\bar{\mathbf{V}}^i_{\boldsymbol{\gamma}}||_2 < \varepsilon$)

a) Set $i = i + 1$.

b) Generate a uniformly random orthogonal matrix [18] $\mathbf{Q}^i$ of dimension $n_x \times n_x$ and a random number ρ^i from the Chi distribution with (n_x+2) degrees of freedom, i.e., $\rho^i \sim \mathrm{Chi}(n_x + 2)$.

c) Compute a set of points $\{\mathbf{x}^i_j\}_{j=0}^{2n_x}$ and appropriate weights $\{\omega^i_j\}_{j=0}^{2n_x}$ according to

$$\mathbf{x}^i_0 = \mathbf{m}, \qquad \omega^i_0 = 1 - \frac{n_x}{(\rho^i)^2}, \tag{19}$$

$$\mathbf{x}^i_{1,\ldots,2n_x} = \mathbf{m} \pm \rho^i \mathbf{S}\mathbf{Q}^i \boldsymbol{\xi}_j, \quad \omega^i_{1,\ldots,2n_x} = \frac{1}{2(\rho^i)^2}, \tag{20}$$

where $j = 1, 2, \ldots, n_x$, $\boldsymbol{\xi}_j$ is the j-th column of the $n_x \times n_x$ identity matrix, and $\mathbf{S}$ is a decomposition of matrix $\mathbf{P}$ such that $\mathbf{P} = \mathbf{S}\mathbf{S}^T$, e.g, Cholesky decomposition for lower triangular $\mathbf{S}$.

d) Compute the following relations for the approximation of the integral value at current iteration $\mathbf{I}^i_{\boldsymbol{\gamma}}$, the updated integral value $\bar{\mathbf{I}}^i$, and the corresponding mean square error estimate $\bar{\mathbf{V}}^i$, i.e.,

$$\mathbf{I}^i_{\boldsymbol{\gamma}}(\mathbf{Q}^i, \rho^i) = \sum_{j=0}^{2n_x} \omega^i_j \boldsymbol{\gamma}(\mathbf{x}^i_j), \tag{21}$$

$$\mathbf{D} = \frac{\mathbf{I}^i_{\boldsymbol{\gamma}}(\mathbf{Q}^i, \rho^i) - \bar{\mathbf{I}}^{i-1}_{\boldsymbol{\gamma}}}{i}, \tag{22}$$

$$\bar{\mathbf{I}}^i_{\boldsymbol{\gamma}} = \bar{\mathbf{I}}^{i-1}_{\boldsymbol{\gamma}} + \mathbf{D}, \tag{23}$$

$$\bar{\mathbf{V}}^i_{\boldsymbol{\gamma}} = \frac{i-2}{i} \bar{\mathbf{V}}^{i-1}_{\boldsymbol{\gamma}} + \mathbf{D}\mathbf{D}^T. \tag{24}$$

Step 4: Once the stopping condition is fulfilled, the approximate value of the integral $\mathbf{I}_{\boldsymbol{\gamma}}$ is $\bar{\mathbf{I}}^i_{\boldsymbol{\gamma}}$ with corresponding mean square error estimate $\bar{\mathbf{V}}^i_{\boldsymbol{\gamma}}$.

Note that the SIR is a combination of stochastic radial and spherical rules, where ρ corresponds to the radial rule and $\mathbf{Q}$ to the spherical rule.

The relation (21) represents a single iteration of the integral evaluation. The total approximate value of the integral is then given by an average over all N iterations

$$\bar{\mathbf{I}}^N_{\boldsymbol{\gamma}} = \frac{1}{N} \sum_{i=1}^{N} \mathbf{I}^i_{\boldsymbol{\gamma}}(\rho^i, \mathbf{Q}^i) = \frac{1}{N} \sum_{i=1}^{N} \sum_{j=0}^{2n_x} \omega^i_j \boldsymbol{\gamma}(\mathbf{x}^i_j), \tag{25}$$

where ω^i_j is the weight of the j-th point $\mathbf{x}^i_j$ at the i-th iteration, where both ω^i_j and $\mathbf{x}^i_j$ depend on the samples ρ^i, and $\mathbf{Q}^i$ of ρ and $\mathbf{Q}$ generated at the i-th iteration.

The **Algorithm 2** also computes an estimate $\bar{\mathbf{V}}^N_{\boldsymbol{\gamma}}$ of the variance of the integral value error $\tilde{\mathbf{I}}^N_{\boldsymbol{\gamma}} \triangleq \mathbf{I}_{\boldsymbol{\gamma}} - \bar{\mathbf{I}}^N_{\boldsymbol{\gamma}}$. The error has zero mean

$$\mathbb{E}\Big[\tilde{\mathbf{I}}^N_{\boldsymbol{\gamma}}\Big] = \mathbf{0} \tag{26}$$

and its CM is

$$\mathbb{E}\Big[\tilde{\mathbf{I}}^N_{\boldsymbol{\gamma}} (\tilde{\mathbf{I}}^N_{\boldsymbol{\gamma}})^T\Big] = \mathbb{V}\Big[\tilde{\mathbf{I}}^N_{\boldsymbol{\gamma}}\Big] = \mathbb{V}\big[\bar{\mathbf{I}}^N_{\boldsymbol{\gamma}}\big]. \tag{27}$$

The SIR estimates the CM by (24) as

$$\mathbb{V}\big[\bar{\mathbf{I}}^N_{\boldsymbol{\gamma}}\big] \approx \bar{\mathbf{V}}^N_{\boldsymbol{\gamma}} \triangleq \frac{1}{N} \mathrm{svar}(\mathbf{I}^{1:N}_{\boldsymbol{\gamma}}), \tag{28}$$

where $\mathrm{svar}(\mathbf{I}^{1:N}_{\boldsymbol{\gamma}})$ is the sample variance over $\mathbf{I}^1_{\boldsymbol{\gamma}}, ..., \mathbf{I}^N_{\boldsymbol{\gamma}}$ as

$$\bar{\mathbf{V}}^N_{\boldsymbol{\gamma}} = \frac{1}{N} \frac{1}{N-1} \sum_{i=1}^{N} \Big(\mathbf{I}^i_{\boldsymbol{\gamma}} - \bar{\mathbf{I}}^N_{\boldsymbol{\gamma}}\Big)\Big(\mathbf{I}^i_{\boldsymbol{\gamma}} - \bar{\mathbf{I}}^N_{\boldsymbol{\gamma}}\Big)^T. \tag{29}$$

D. Problem formulation

Due to the nature of the SIR, the integral value $\mathbf{I}_{\boldsymbol{\gamma}}$ is approximated by a random variable $\bar{\mathbf{I}}^N_{\boldsymbol{\gamma}}$ which has mean equal to $\mathbf{I}_{\boldsymbol{\gamma}}$ and the CM given by $\mathbb{V}\big[\bar{\mathbf{I}}^N_{\boldsymbol{\gamma}}\big]$ is approximated by $\bar{\mathbf{V}}^N_{\boldsymbol{\gamma}}$.

First, the SIF algorithm should properly reflect the fact that the moments (13) – (17) are computed using random integral

[3]Weighted points will be denoted as sigma-points, even though this term is usually reserved for weighted points of the UKF.

values. Up to now, no analysis of this fact and its influence on the SIF algorithm was made. The analysis should be primarily concerned with bias aspects of the computed moments.

Second, the implementation aspects should be investigated. It is well known that the Monte Carlo techniques are computationally demanding. Even thought the SIR converges faster than perfect Monte Carlo [17], its properties are likewise derived for $N \to \infty$. The principal source of computational demands is the propagation of large quantities of sigma-points, which goes hand in hand with generating samples of ρ and random orthogonal matrices $\mathbf{Q}$. This is quite impractical, therefore there is a strong demand for reducing the number of iterations N as much as possible.

III. Theoretical Aspects

Now, the influence of random evaluations of the integrals in the SIF algorithm will be analyzed. For convenience, the following notation further distinguishes variants of the general moment integral (18), in particular $\boldsymbol{\gamma}(\mathbf{x}) = \mathbf{g}(\mathbf{x}), \boldsymbol{\gamma}(\mathbf{x}) = \mathbf{g}(\mathbf{x})\mathbf{g}^T(\mathbf{x})$, and $\boldsymbol{\gamma}(\mathbf{x}) = \mathbf{x}\mathbf{g}^T(\mathbf{x})$ for evaluating mean, second non-central moment, and cross-covariance will be used, i.e.,

$$\mathbf{I}_{\mathbf{g}} \triangleq \int \mathbf{g}(\mathbf{x})\, \mathcal{N}\{\mathbf{x}; \mathbf{m}, \mathbf{P}\}\, \mathrm{d}\mathbf{x}, \tag{30}$$

$$\mathbf{I}_{\mathbf{gg}} \triangleq \int \mathbf{g}(\mathbf{x})\mathbf{g}^T(\mathbf{x})\, \mathcal{N}\{\mathbf{x}; \mathbf{m}, \mathbf{P}\}\, \mathrm{d}\mathbf{x}, \tag{31}$$

$$\mathbf{I}_{\mathbf{xg}} \triangleq \int \mathbf{x}\mathbf{g}^T(\mathbf{x})\mathcal{N}\{\mathbf{x}; \mathbf{m}, \mathbf{P}\}\, \mathrm{d}\mathbf{x}. \tag{32}$$

A further extension of this notation leads to the degree 3 SIR estimate $\bar{\mathbf{I}}_{\mathbf{g}}$ of $\mathbf{I}_{\mathbf{g}}$ with its integral error estimate $\bar{\mathbf{V}}_{\mathbf{g}}$, degree 3 SIR estimate $\bar{\mathbf{I}}_{\mathbf{gg}}$ of $\mathbf{I}_{\mathbf{gg}}$ with its integral error estimate $\bar{\mathbf{V}}_{\mathbf{gg}}$, and degree 3 SIR estimate $\bar{\mathbf{I}}_{\mathbf{xg}}$ of $\mathbf{I}_{\mathbf{xg}}$ with its integral error estimate $\bar{\mathbf{V}}_{\mathbf{xg}}$. Note that the superscript N denoting the number of iterations is omitted for convenience.

A. Stochastic Integration for Moment Transform

Now, an analysis of moments of a transformed random variable computed via SIR will be made. Note that in the algorithm of the SIF, three types of moments have to be calculated, in particular:

- The mean value integrals of (13) and (16) in the form of $\mathbb{E}[\mathbf{g}(\mathbf{x})]$, where $\mathbf{g}(\mathbf{x}) = \mathbf{h}_k(\mathbf{x}_k)$ or $\mathbf{g}(\mathbf{x}) = \mathbf{f}_k(\mathbf{x}_k)$.
- the variance integrals (14) and (17) in the form of the integral $\mathbb{V}[\mathbf{g}(\mathbf{x})]$, where $\mathbf{g}(\mathbf{x}) = \mathbf{h}_k(\mathbf{x}_k)$ or $\mathbf{g}(\mathbf{x}) = \mathbf{f}_k(\mathbf{x}_k)$.
- the cross-covariance integral (15) in the form of the integral $\mathbb{C}[\mathbf{x}, \mathbf{g}(\mathbf{x})]$, where $\mathbf{g}(\mathbf{x}) = \mathbf{h}_k(\mathbf{x}_k)$.

The analysis will deal with moments $\mathbb{E}[\mathbf{y}], \mathbb{V}[\mathbf{y}]$, and $\mathbb{C}[\mathbf{x}, \mathbf{y}]$ of the transformed variable $\mathbf{y} = \mathbf{g}(\mathbf{x})$ for $\mathbf{x} \sim \mathcal{N}\{\mathbf{x}; \mathbf{m}, \mathbf{P}\}$.

1) The Mean Value: The mean value of the transformed variable $\mathbf{y}$ is defined as $\mathbb{E}[\mathbf{y}] = \mathbf{I}_{\mathbf{g}} = \int \mathbf{g}(\mathbf{x})\, \mathcal{N}\{\mathbf{x}; \mathbf{m}, \mathbf{P}\}\, \mathrm{d}\mathbf{x}$, which is approximated by the SIR as

$$\mathbb{E}[\mathbf{y}] \approx \widehat{\mathbb{E}[\mathbf{y}]} = \widehat{\mathbb{E}[\mathbf{g}(\mathbf{x})]} = \bar{\mathbf{I}}_{\mathbf{g}}. \tag{33}$$

The SIR is constructed in such way that the estimates are unbiased $\mathbb{E}\Big[\widehat{\mathbb{E}[\mathbf{g}(\mathbf{x})]}\Big] = \mathbf{0}$, where $\widetilde{\mathbb{E}[\mathbf{g}(\mathbf{x})]} \triangleq \mathbb{E}[\mathbf{g}(\mathbf{x})] - \widehat{\mathbb{E}[\mathbf{g}(\mathbf{x})]}$. Hence, it holds

$$\mathbb{E}\Big[\widehat{\mathbb{E}[\mathbf{y}]}\Big] = \mathbb{E}\Big[\widehat{\mathbb{E}[\mathbf{g}(\mathbf{x})]}\Big] = \mathbf{I}_{\mathbf{g}} = \mathbb{E}[\mathbf{y}]. \tag{34}$$

2) The Variance: The CM of the transformed variable $\mathbf{y}$ is defined as

$$\mathbb{V}[\mathbf{y}] = \mathbb{E}\big[(\mathbf{y} - \mathbb{E}[\mathbf{y}])(\mathbf{y} - \mathbb{E}[\mathbf{y}])^T\big] = \mathbf{I}_{\mathbf{gg}} - \mathbf{I}_{\mathbf{g}}\mathbf{I}_{\mathbf{g}}^T, \tag{35}$$

which can be approximated by the SIR as

$$\mathbb{V}[\mathbf{y}] \approx \widehat{\mathbb{V}[\mathbf{y}]} = \widehat{\mathbb{V}[\mathbf{g}(\mathbf{x})]} = \mathbb{E}[\widehat{\mathbf{g}(\mathbf{x})\mathbf{g}^T(\mathbf{x})}] - \widehat{\mathbb{E}[\mathbf{g}(\mathbf{x})]}\widehat{\mathbb{E}[\mathbf{g}(\mathbf{x})]}^T.$$

Now, the unbiasedness of $\widehat{\mathbb{V}[\mathbf{y}]}$ will be analyzed:

$$\begin{aligned}
\mathbb{E}\Big[\widehat{\mathbb{V}[\mathbf{y}]}\Big] &= \mathbb{E}\Big[\mathbb{E}[\widehat{\mathbf{g}(\mathbf{x})\mathbf{g}^T(\mathbf{x})}]\Big] \\
&\quad - \mathbb{E}\left[\Big(\underbrace{\widehat{\mathbb{E}[\mathbf{g}(\mathbf{x})]} - \mathbb{E}[\mathbf{g}(\mathbf{x})]}_{\widetilde{\mathbb{E}[\mathbf{g}(\mathbf{x})]}} + \mathbb{E}[\mathbf{g}(\mathbf{x})]\Big)\Big(\,\cdot\,\Big)^T\right] \\
&= \mathbb{E}\big[\mathbf{g}(\mathbf{x})\mathbf{g}^T(\mathbf{x})\big] - \mathbb{E}[\mathbf{g}(\mathbf{x})]\mathbb{E}[\mathbf{g}(\mathbf{x})]^T - \mathbb{E}\Big[\widetilde{\mathbb{E}[\mathbf{g}(\mathbf{x})]}\widetilde{\mathbb{E}[\mathbf{g}(\mathbf{x})]}^T\Big] \\
&= \mathbf{I}_{\mathbf{gg}} - \mathbf{I}_{\mathbf{g}}\mathbf{I}_{\mathbf{g}}^T - \mathbf{V}_{\mathbf{g}},
\end{aligned} \tag{36}$$

i.e., by comparing (35) and (36), the estimate $\widehat{\mathbb{V}[\mathbf{y}]}$ is biased by $\mathbf{V}_{\mathbf{g}}$.

The unbiased SIR estimate of $\mathbb{V}[\mathbf{y}]$ denoted as $\widehat{\mathbb{V}[\mathbf{y}]}^*$ should thus be computed by

$$\begin{aligned}
\widehat{\mathbb{V}[\mathbf{y}]}^* &= \mathbb{E}[\widehat{\mathbf{g}(\mathbf{x})\mathbf{g}^T(\mathbf{x})}] - \widehat{\mathbb{E}[\mathbf{g}(\mathbf{x})]}\widehat{\mathbb{E}[\mathbf{g}(\mathbf{x})]}^T + \bar{\mathbf{V}}_{\mathbf{g}} \\
&= \bar{\mathbf{I}}_{\mathbf{gg}} - \bar{\mathbf{I}}_{\mathbf{g}}\bar{\mathbf{I}}_{\mathbf{g}}^T + \bar{\mathbf{V}}_{\mathbf{g}}.
\end{aligned} \tag{37}$$

3) The Cross-Covariance: The cross-covariance matrix of the random variables $\mathbf{x}$ and $\mathbf{y}$ is defined as

$$\mathbb{C}[\mathbf{x}, \mathbf{y}] = \mathbb{E}\big[(\mathbf{x} - \mathbb{E}[\mathbf{x}])(\mathbf{y} - \mathbb{E}[\mathbf{y}])^T\big] = \mathbf{I}_{\mathbf{xg}} - \mathbf{m}\mathbf{I}_{\mathbf{g}}^T, \tag{38}$$

which can be approximated by the SIR as

$$\begin{aligned}
\mathbb{C}[\mathbf{x}, \mathbf{y}] &\approx \widehat{\mathbb{C}[\mathbf{x}, \mathbf{y}]} = \widehat{\mathbb{C}[\mathbf{x}, \mathbf{g}(\mathbf{x})]} = \mathbb{E}[\widehat{\mathbf{x}\mathbf{g}^T(\mathbf{x})}] - \mathbb{E}[\mathbf{x}]\widehat{\mathbb{E}[\mathbf{g}(\mathbf{x})]}^T \\
&= \bar{\mathbf{I}}_{\mathbf{xg}} - \mathbf{m}\bar{\mathbf{I}}_{\mathbf{g}}^T.
\end{aligned} \tag{39}$$

To analyze unbiasedness of (39), the mean value of $\widehat{\mathbb{C}[\mathbf{x}, \mathbf{y}]}$ is computed as

$$\begin{aligned}
\mathbb{E}\Big[\widehat{\mathbb{C}[\mathbf{x}, \mathbf{y}]}\Big] &= \mathbb{E}\Big[\widehat{\mathbb{E}[\mathbf{x}\mathbf{g}^T(\mathbf{x})]}\Big] - \mathbb{E}\Big[\mathbb{E}[\mathbf{x}]\widehat{\mathbb{E}[\mathbf{g}(\mathbf{x})]})^T\Big] \\
&= \mathbb{E}\big[\mathbf{x}\mathbf{g}^T(\mathbf{x})\big] - \mathbb{E}[\mathbf{x}]\mathbb{E}[\mathbf{g}(\mathbf{x})]^T = \mathbf{I}_{\mathbf{xg}} - \mathbf{m}\mathbf{I}_{\mathbf{g}}^T,
\end{aligned} \tag{40}$$

The SIR estimate (39) is an unbiased estimate of $\mathbb{C}[\mathbf{x}, \mathbf{y}]$.

B. SIF Innovation Sequence Properties

Now, the properties of the innovation sequence $\tilde{\mathbf{z}}_{k|k-1} \triangleq \mathbf{z}_k - \hat{\mathbf{z}}_{k|k-1}$ appearing in (10) and especially its variance in (14) will be analyzed. For convenience, the time indices are omitted in the analysis. The mean value of $\tilde{\mathbf{z}}$ is

$$\mathbb{E}[\tilde{\mathbf{z}}] = \mathbb{E}[\mathbf{z} - \hat{\mathbf{z}}] = \mathbb{E}[\mathbf{z}] - \mathbb{E}[\mathbf{z}] = \mathbf{0}, \tag{41}$$

whereas the variance of $\tilde{\mathbf{z}}$ is

$$\begin{aligned}\mathbb{V}[\tilde{\mathbf{z}}] &= \mathbb{E}\big[(\tilde{\mathbf{z}}-\mathbb{E}[\tilde{\mathbf{z}}])(\tilde{\mathbf{z}}-\mathbb{E}[\tilde{\mathbf{z}}])^T\big] = \mathbb{E}\big[\tilde{\mathbf{z}}\tilde{\mathbf{z}}^T\big] \\ &= \mathbb{E}\big[(\mathbf{z}-\hat{\mathbf{z}})(\mathbf{z}-\hat{\mathbf{z}})^T\big] = \mathbb{E}\big[\mathbf{z}\mathbf{z}^T\big] - \mathbb{E}[\hat{\mathbf{z}}]\mathbb{E}[\hat{\mathbf{z}}]^T \\ &= \mathbb{E}\big[\mathbf{z}\mathbf{z}^T\big] - \mathbb{E}[\mathbf{z}]\mathbb{E}[\mathbf{z}]^T = \mathbf{P}^{\mathbf{zz}}. \end{aligned} \tag{42}$$

Now, the innovation sequence of the SIF, where the moment $\hat{\mathbf{z}}$ is calculated according to (33) and denoted as $\widehat{\mathbb{E}[\mathbf{z}]}$ will be analyzed. The mean value of the innovation $\mathbf{z}-\widehat{\mathbb{E}[\mathbf{z}]}$ is

$$\mathbb{E}\Big[\mathbb{E}\Big[\mathbf{z}-\widehat{\mathbb{E}[\mathbf{z}]}\Big]\Big] = \mathbb{E}[\mathbf{z}]-\mathbb{E}[\mathbf{z}] = \mathbf{0}, \tag{43}$$

but this time the variance of the innovation sequence is

$$\begin{aligned}&\mathbb{V}\Big[\mathbf{z}-\widehat{\mathbb{E}[\mathbf{z}]}\Big] = \mathbb{E}\Big[(\mathbf{z}-\widehat{\mathbb{E}[\mathbf{z}]})(\mathbf{z}-\widehat{\mathbb{E}[\mathbf{z}]})^T\Big] \\ &= \mathbb{E}\big[\mathbf{z}\mathbf{z}^T\big] - \mathbb{E}\Big[\mathbf{z}\,\widehat{\mathbb{E}[\mathbf{z}]}^T\Big] - \mathbb{E}\Big[\widehat{\mathbb{E}[\mathbf{z}]}\mathbf{z}^T\Big] + \mathbb{E}\Big[\widehat{\mathbb{E}[\mathbf{z}]}\widehat{\mathbb{E}[\mathbf{z}]}^T\Big] \\ &= \mathbb{E}\big[\mathbf{z}\mathbf{z}^T\big] - 2\mathbb{E}[\mathbf{z}]\mathbb{E}[\mathbf{z}]^T + \mathbb{E}\Big[\widehat{\mathbb{E}[\mathbf{z}]}\Big]\mathbb{E}\Big[\widehat{\mathbb{E}[\mathbf{z}]}\Big]^T + \mathbb{V}\Big[\widehat{\mathbb{E}[\mathbf{z}]}\Big] \\ &= \mathbb{E}\big[\mathbf{z}\mathbf{z}^T\big] - \mathbb{E}[\mathbf{z}]\mathbb{E}[\mathbf{z}]^T + \mathbb{V}\Big[\widehat{\mathbb{E}[\mathbf{z}]}\Big] = \mathbf{P}^{\mathbf{zz}} + \mathbb{V}\Big[\widehat{\mathbb{E}[\mathbf{z}]}\Big]. \end{aligned} \tag{44}$$

Thus, the variance of the innovation sequence of the SIF (44) is by term $\mathbb{V}\Big[\widehat{\mathbb{E}[\mathbf{z}]}\Big]$ higher compared to innovation sequence variance of the GF (42). This should be reflected by the Kalman gain and $\mathbf{K}_k$ in (12) should be replaced in the SIF by

$$\mathbf{K}_k^* = \mathbb{C}[\mathbf{x}_k, \widehat{\mathbf{z}_k|\mathbf{z}^{k-1}}]\Big(\mathbb{V}[\widehat{\mathbf{z}_k|\mathbf{z}^{k-1}}] + \mathbb{V}\Big[\widehat{\mathbb{E}[\mathbf{z}_k|\mathbf{z}^{k-1}]}\Big]\Big)^{-1}. \tag{45}$$

IV. Implementation Aspects

This section deals with implementation aspects, where in particular a truncated radial rule will be proposed and several ways to reduce computational costs of the SIF will be discussed.

Recall that the moments (13) – (17) can be calculated using the SIR and the results derived in Sec. III as follows.

The measurement update moments are approximated by

$$\hat{\mathbf{z}}_{k|k-1} \approx \bar{\mathbf{I}}_{\mathbf{h}_k}, \tag{46}$$

$$\mathbf{P}^{\mathbf{xz}}_{k|k-1} \approx \bar{\mathbf{I}}_{\mathbf{x}\mathbf{h}_k} - \hat{\mathbf{x}}_{k|k-1}\bar{\mathbf{I}}^T_{\mathbf{h}_k}, \tag{47}$$

$$\mathbf{P}^{\mathbf{zz}}_{k|k-1} \approx \bar{\mathbf{I}}_{\mathbf{h}_k\mathbf{h}_k} - \bar{\mathbf{I}}_{\mathbf{h}_k}\bar{\mathbf{I}}^T_{\mathbf{h}_k} + 2\bar{\mathbf{V}}_{\mathbf{h}_k}, \tag{48}$$

where term (48) stems from (36) and (44).

The time update moments are approximated by

$$\hat{\mathbf{x}}_{k+1|k} \approx \bar{\mathbf{I}}_{\mathbf{f}_k}, \tag{49}$$

$$\mathbf{P}^{\mathbf{xx}}_{k+1|k} \approx \bar{\mathbf{I}}_{\mathbf{f}_k\mathbf{f}_k} - \bar{\mathbf{I}}_{\mathbf{f}_k}\bar{\mathbf{I}}^T_{\mathbf{f}_k} + \bar{\mathbf{V}}_{\mathbf{f}_k}. \tag{50}$$

Note that approximated second moments (47), (48) and (50) can also be calculated directly as central moments, e.g.,

$$\bar{\mathbf{I}}_{\mathbf{x}\mathbf{h}_k} - \hat{\mathbf{x}}_{k|k-1}\bar{\mathbf{I}}^T_{\mathbf{h}_k} = \bar{\mathbf{I}}_{(\mathbf{x}-\hat{\mathbf{x}}_{k|k-1})(\mathbf{h}_k-\bar{\mathbf{I}}_{\mathbf{h}_k})}, \tag{51}$$

$$\bar{\mathbf{I}}_{\mathbf{h}_k\mathbf{h}_k} - \bar{\mathbf{I}}_{\mathbf{h}_k}\bar{\mathbf{I}}^T_{\mathbf{h}_k} = \bar{\mathbf{I}}_{(\mathbf{h}_k-\bar{\mathbf{I}}_{\mathbf{h}_k})(\mathbf{h}_k-\bar{\mathbf{I}}_{\mathbf{h}_k})}. \tag{52}$$

A. Truncated Radial Rule

In the SIF, three types of integrals are evaluated to obtain state and measurement predictive moments:

The mean value integrals (46) and (49), the values are $n_x \times 1$ or $n_z \times 1$ vectors.

The cross-covariance integral (47), the values are $n_x \times n_z$ matrices.

The variance integrals (48) and (50), the values are $n_x \times n_x$ or $n_z \times n_z$ matrices.

While the mean value and cross-covariance integrals can attain arbitrary values, the variance integrals must be positive definite. This is critical especially when using small number of iterations N as the integral error variance $\mathbf{V}_{\mathbf{gg}}$ could be large for such N and the approximate variance (37) may be negative definite. The numerical rules do not generally guarantee the positive definiteness of variance integrals for finite N. By rearranging the variance computation in accordance with (52) the pitfall becomes obvious. The positive definiteness of the approximate variance integral depends on the weighting by ω. In fact, in case of the degree 3 SIR it depends on the central sigma-point weighting ω_0^i.

Note that similar problem arises in the UKF, which can be viewed as a single iteration of the SIF with $\mathbf{Q}$ being the identity matrix and fixed $\rho = \sqrt{n_x + \kappa}$ [16]. The problem is usually solved by restricting $\kappa = \max(0, 3 - n_x)$, i. e., by guaranteeing non-negativeness of ω_0 [19], [20].

Hence, a similar approach is proposed: i) to calculate the variance integral directly as central moment (52) and ii) to constrain the parameter $\rho \sim \mathrm{Chi}_d$ with $d = n_x + 2$ degrees of freedom to avoid negative ω_0. Note that ρ corresponds to the radial rule of the SIR.

The equation (19) and the condition $\omega_0 \geq 0$ imply that $\rho \geq \sqrt{n_x}$. Thus, ρ should be generated from a truncated Chi distribution preserving the mean of the Chi distribution. Thus, we propose a truncated Chi distribution to generate the radial rule parameter ρ, where the lower bound is given by $\underline{\rho} = \sqrt{n_x}$ and the upper bound $\overline{\rho}$ can be easily inferred from

$$\int_{-\infty}^{\infty} x f_d(x)\mathrm{d}x = \frac{1}{F_d(\overline{\rho}) - F_d(\underline{\rho})}\int_{\underline{\rho}}^{\overline{\rho}} x f_d(x)\mathrm{d}x,$$

where $f_d(x)$ is the PDF and $F_d(\cdot)$ is the cumulative density function of Chi_d distribution with d degrees of freedom.

The generation is described in Algorithm 3.

Algorithm 3 Generating a sample from the Truncated Chi distribution $\mathrm{Chi}_d^T(\underline{\rho})$

Step 1: Find $\overline{\rho}$ from $F_d(\overline{\rho}) - F_d(\underline{\rho}) = F_{d+1}(\overline{\rho}) - F_{d+1}(\underline{\rho})$.

Step 2: Generate a uniformly random $u \sim \mathrm{U}(F_d(\underline{\rho}), F_d(\overline{\rho}))$.

Step 3: Using inverse Chi distribution function, transform u into desired truncated Chi distribution $\rho = F_d^{-1}(u)$. Then, $\rho \sim \mathrm{Chi}_d^T(\underline{\rho})$.

To illustrate the properties of the truncated Chi distribution with three degrees of freedom ($n_x = 1$), Fig. 1 is presented.

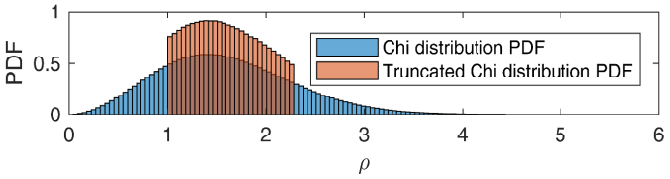


Fig. 1. Chi and truncated Chi PDFs with three degrees of freedom.

B. Reduction of Computational Costs

The SIF employing the SIR is computationally demanding, therefore efforts to reduce the costs are important. There are several simple approaches.

First, a trivial approach is to reduce the number of iterations N. However a combination of small N and a highly nonlinear function may lead to negative definite approximate variance integral. A technique to avoid such negative definiteness has been introduced in the previous section.

Second, generating random orthogonal matrices $\mathbf{Q}$ is very costly, thus generating these matrices and random ρ can be performed off-line.

Third, separate computation of the moments (13), (14), and (15) at a measurement update step requires three runs of Algorithm 2. The computation of the integrals in a single run of the SIR with shared sigma-points $\mathbf{x}_j^i$ and weights ω_j^i will significantly reduce the costs as the propagation of sigma-points through nonlinear function is usually the most computationally demanding operation. The same idea can be applied for (16) and (17) at a time update step.

V. Numerical Illustrations

The numerical illustrations consist of three examples illustrating performance of the SIF with modifications proposed in Sections III and IV. Particularly, the first static example involving functions used for modeling sensors in target tracking demonstrates improvements of the SIR with small N by using the truncated Chi distribution. The second static example of mapping polar to Cartesian coordinates illustrates usage of the truncated Chi distribution for the SIR (denoted as truncated SIR) with small N and reduction of computational costs by using shared sigma-points for the SIR with large N. Finally, the improved performance of the SIF implementing the recommendations proposed in Sec. IV will be illustrated using a dynamic example of bearings-only tracking.

A. Static Examples of Sensor Models

In this example, we illustrate instability of the SIR for a very small number of iterations N and stability improvement induced by the truncated distribution. For the illustration, three functions appearing in sensor models for target tracking were selected. These are in particular: range, bearing, and received signal strength.

In three test scenarios, a random variable with Gaussian distribution $\mathcal{N}\{\mathbf{x}; \mathbf{m}, \mathbf{P}\}$ is propagated through the selected nonlinear functions $y = \mathbf{g}(\mathbf{x})$. The nonlinear function $\mathbf{g}(\mathbf{x})$ and a priori information $\mathbf{m}$ and $\mathbf{P}$ are defined in the Table I.

TABLE I
Results of the static tests.

Filter	$\mathbb{E}[\widehat{\mathbb{V}[y]}]$	mean squared error of $\widehat{\mathbb{V}[y]}$
Scenario 1		
$m = [3,0]^T, \mathbf{P} = \mathrm{diag}(10,100), y = \sqrt{x_1^2 + x_2^2}$		
Ground truth	31.0	
Unscented transform	43.6	
$10^6 \times \mathrm{SIR}_{\mathrm{standard}}(N=10)$	31.4	131.4
$10^6 \times \mathrm{SIR}_{\mathrm{truncated}}(N=10)$	38.6	78.2
Scenario 2		
$m = [3,0]^T, \mathbf{P} = \mathrm{diag}(10,1), y = \arctan(x_1, x_2)$		
Ground truth	1.32	
Unscented transform	1.46	
$10^6 \times \mathrm{SIR}_{\mathrm{standard}}(N=10)$	1.33	0.046
$10^6 \times \mathrm{SIR}_{\mathrm{truncated}}(N=10)$	1.47	0.033
Scenario 3		
$m = [0.1,0.1]^T, \mathbf{P} = \mathrm{diag}(0.1,0.1), y = 10 - 20\log_{10}(x_1^2 + x_2^2)$		
Ground truth	123.7	
Unscented transform	129.6	
$10^6 \times \mathrm{SIR}_{\mathrm{standard}}(N=10)$	129.0	9291
$10^6 \times \mathrm{SIR}_{\mathrm{truncated}}(N=10)$	154.9	1389

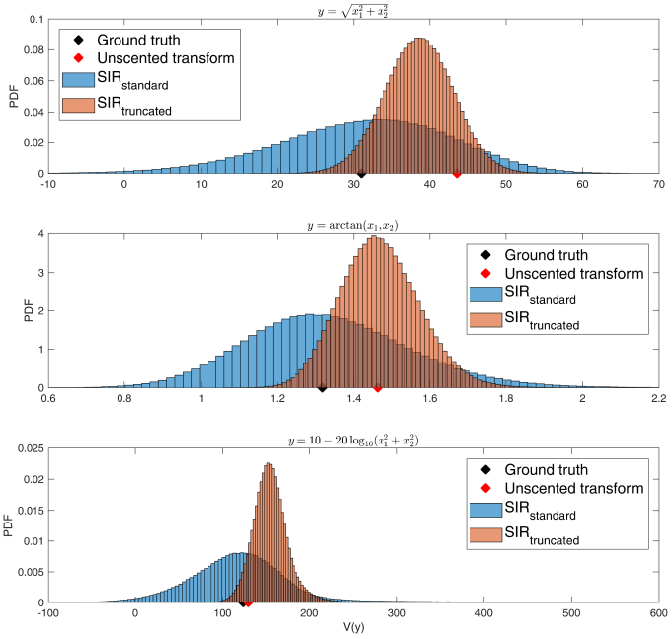


Fig. 2. Static examples of sensor models; histograms of variance integral estimates for different nonlinearities.

In each scenario, the standard SIR and the truncated SIR were employed, both with $N = 10$. To obtain an idea of their estimate statistics, both rules were tested in 10^6 independent Monte Carlo runs. Also, the perfect Monte Carlo transform (with $5 \cdot 10^7$ iterations) to obtain the ground truth and the unscented transform (with $\kappa = 1$) for a comparison with a simpler transform were performed. The results are summarized in Table I and Figure 2.

A biasedness of the truncated SIR is obvious, but especially in scenarios 1 and 3, the standard SIR provides negative approximate variance integral values (0.72 % of variance estimates in test scenario 1 and in test scenario 3 even 1.62 %

of variance estimates). In addition, in all cases the mean squared error of the estimates is significantly higher for the standard SIR compared to the truncated SIR.

B. Mapping from Polar to Cartesian Coordinates

The conversion from polar to Cartesian coordinates [21] is a ubiquitous nonlinearity appearing in radar sensors or laser range finders and is given by

$$\begin{bmatrix} x \\ y \end{bmatrix} = \begin{bmatrix} r\cos(\theta) \\ r\sin(\theta) \end{bmatrix}. \tag{53}$$

We compared the performance of the standard SIR and the truncated SIR for $N = 5$ and performance of the standard SIR with and without shared sigma-points for $N = 50$. Both test cases were made for 100 different a priori moments. The 10 different positions on a spiral in polar coordinates were chosen as input mean $\mathbf{m}_i = [r_i, \theta_i]$. For each mean 10 different input CMs $\mathbf{P} = \mathrm{diag}([\sigma_r^2, \sigma_{\theta,j}^2])$ were assigned. Standard deviation of range was $\sigma_r = 0.5\,\mathrm{m}$ and azimuth standard deviations were uniformly placed in the interval $\sigma_{\theta,j}^2 \in [6°, 33°]$ for $j = 1, .., 10$. Figure 3 depicts the input means in polar coordinates. As a measure of agreement between the approximate moments

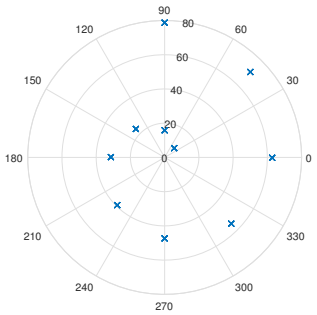


Fig. 3. Input means are placed on a spiral. For each input mean $\mathbf{m}_i = [r_i \theta_i]$ (blue cross) the radius variance is fixed at $\sigma_r = 0.5\,\mathrm{m}$ and 10 different azimuth variances are considered so that $\sigma_\theta \in [6°, 33°]$.

$(\widehat{\mathbb{E}[\mathbf{y}]}, \widehat{\mathbb{V}[\mathbf{y}]})$ and the ground truth moments $(\mathbb{E}[\mathbf{y}], \mathbb{V}[\mathbf{y}])$ we used the symmetrized Kullback-Leibler divergence (SKL) of the Gaussian densities given by

$$\begin{aligned} \mathrm{SKL} = \frac{1}{4}\Big[&(\mathbb{E}[\mathbf{y}] - \widehat{\mathbb{E}[\mathbf{y}]})^T \mathbb{V}[\mathbf{y}]^{-1} (\mathbb{E}[\mathbf{y}] - \widehat{\mathbb{E}[\mathbf{y}]}) \\ &+ (\widehat{\mathbb{E}[\mathbf{y}]} - \mathbb{E}[\mathbf{y}])^T \widehat{\mathbb{V}[\mathbf{y}]}^{-1} (\widehat{\mathbb{E}[\mathbf{y}]} - \mathbb{E}[\mathbf{y}]) \\ &+ \mathrm{tr}(\mathbb{V}[\mathbf{y}]^{-1} \widehat{\mathbb{V}[\mathbf{y}]}^{-1} + \mathrm{tr}(\widehat{\mathbb{V}[\mathbf{y}]}^{-1} \mathbb{V}[\mathbf{y}]^{-1}) - 2n_y\Big]. \end{aligned} \tag{54}$$

The ground truth transformed mean and CM were computed using the Monte Carlo method with 10^7 samples. The SKL scores were grouped in two ways; over means and over azimuth variances. The comparison of the standard SIR and the truncated SIR for $N = 5$ is depicted in Fig. 4. The results are shown in the form of a box plot from $2 \cdot 10^4$ independent Monte Carlo simulations. The superior performance of the truncated SIR compared to the standard SIR is obvious, because the outliers of the standard SIR i) reach negative SKL implying negative variance estimates or ii) reach SKL

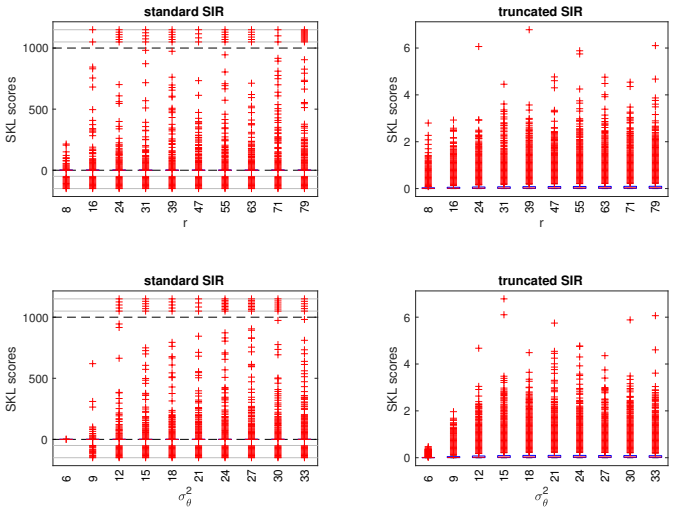


Fig. 4. Mapping polar to Cartesian Coordinates, standard SIR vs. truncated SIR for $N = 5$.

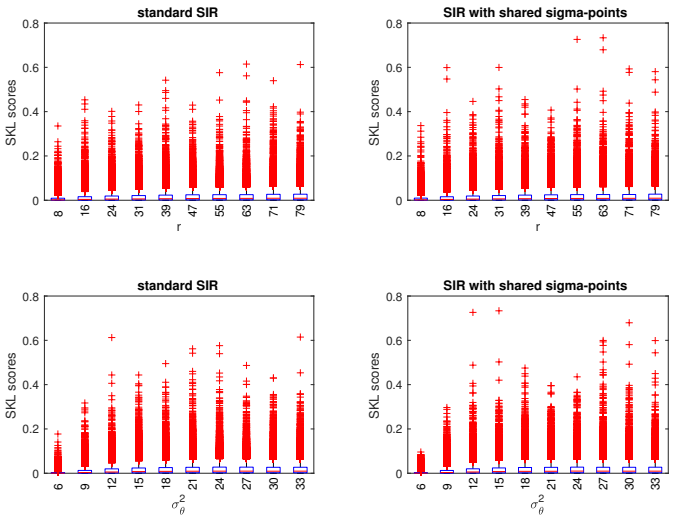


Fig. 5. Mapping polar to Cartesian Coordinates, standard SIR vs. SIR with shared sigma-points for computation of moments for $N = 50$.

higher in order of two magnitudes. The comparison of the standard SIR for computing moments and the SIR with shared sigma-points for $N = 50$ is depicted in Fig. 5. The results are illustrated in the form of a box plot from $2 \cdot 10^3$ independent Monte Carlo simulations. It can be seen that, there is no significant difference between the SIR with shared sigma-points for computation of moments and the standard SIR. The computation demands of two separate algorithms of the SIR are approximately twice compared to the shared sigma-point SIR algorithm.

C. Bearings-Only Tracking

In this example [22], the state of the object will be given by its position in the xy-plane. The object will move along a line parallel to the x axis with its speed proportional to its x position, i.e., $\mathbf{x}_{k+1} = \left[\begin{smallmatrix} 0.9 & 0 \\ 0 & 1 \end{smallmatrix}\right]\mathbf{x}_k + \mathbf{w}_k$ with CM of the state

TABLE II
RESULTS OF THE DYNAMIC TEST.

Filter	% of failures	median of MSE	median of ANEES
Standard SIF	0.085	0.9102	2.3264
Standard SIF with corrections	0.026	0.9102	2.3250
Truncated SIF with corrections	0	0.9080	2.3163

noise $\mathbf{\Sigma}_k^{\mathbf{w}} = \left[\begin{smallmatrix} 0.1 & 0.01 \\ 0.01 & 0.1 \end{smallmatrix}\right]$. The platform moves along a unit circle centered at the origin in order to make the problem observable. The bearing from the platform to the object is measured, i.e., $z_k = \arctan(x_{2,k} - \sin(k), x_{1,k} - \cos(k))$, the translational noises are neglected and the variance of the measurement noise is $\Sigma_\theta^v = 0.025$. The initial condition $\mathbf{x}_0$ is given by $p(\mathbf{x}_0) = \mathcal{N}\{\mathbf{x}_0; [20, 5]^T, \mathrm{diag}([0.1, 0.1])\}$ and the motion of the object was simulated for $k = 0, 1, ..., 50$.

In Table II, the results of 10^5 independent Monte Carlo simulations of the standard SIF, the standard SIF with correction suggested in Sec. III, and the truncated SIF with the corrections both for $N = 10$ are given.

First, as the first column of Table II suggests, the standard SIF diverged in several Monte Carlo simulations due to negative definiteness of either $P_{k|k-1}^{zz}$ or $\mathbf{P}_{k|k}^{\mathbf{xx}}$. The same inconvenient behavior was observed for the standard SIF with the corrections, but at a lower rate. As expected, the truncated SIF with corrections always delivered the desired result.

Second, albeit further analysis might be redundant due to divergence of the standard SIFs, the following approach was adopted. For each trajectory, the mean square error (MSE) and the average normalized estimation error squared (ANEES) were computed. Median value of the MSE and the ANEES are given in Tab. II. The results show that the corrections from Sec. III slightly improve the robustness and the performance in terms of ANEES of the SIF. The truncated SIF (applied results from Sec. III and Sec. IV) was proven to deliver robust results with better performance in terms of MSE and ANEES.

D. Summary of Numerical Illustrations

First, the truncated SIR helps securing positive definiteness of variance integral estimates, thus improving the quality of estimates for a small number N of SIR iterations.

Second, for large N computational demands can be significantly lowered by using common sigma-points for all moments at given time/measurement update step of the SIF.

Third, improved variance integral estimates and respecting increased variance of the innovation sequence connected with the use of the SIR leads to better estimates. Note that this technique is useful for a small number of SIR iterations and the influence of this improvement diminishes with N increasing.

VI. CONCLUSION

The paper dealt with state estimation of discrete-time dynamic stochastic systems by the stochastic integration filter. A special attention was paid to computational and theoretical aspects tied with the fact that the filter uses a stochastic integration rule to calculate state and measurement predictive moments. The nice theoretical property of the rule, which is asymptotically exact result, is paid by high computational costs in comparison with deterministic integration rules. The costs can be reduced by using only a small number of iterations of the rule. For such cases, the theoretical analysis revealed that the computation of the variances should take into account the uncertainty in the computed mean. Also, a technique based on a truncated radial parameter was proposed to ensure positive definite variances computed by the rule with a small number of iterations. If, on the other hand, a large number of iterations is used, a technique based on sharing the sigma-points to reduce the costs was proposed in the paper. Improved performance of the rule and, in consequence, of the filter was demonstrated using static and dynamic examples.

REFERENCES

[1] S. Haykin *et al.*, *Adaptive Signal Processing: Next Generation Solutions*. John Wiley & Sons, 2010, vol. 55.

[2] E. Blasch and D. Kahler, "Multiresolution EO/IR target track and ID," in *SIF Proc. Fusion05*, 2005.

[3] J. Crassidis, "Sigma-point Kalman filtering for integrated GPS and inertial navigation," *Aerospace and Electronic Systems, IEEE Transactions on*, vol. 42, no. 2, pp. 750–756, 2006.

[4] R. Isermann, *Fault-diagnosis systems: an introduction from fault detection to fault tolerance*. Springer Science & Business Media, 2006.

[5] D. P. Bertsekas, *Dynamic Programming and Optimal Control (2 Vol Set)*, 3rd ed. Athena Scientific, 2007.

[6] H. W. Sorenson, "On the development of practical nonlinear filters," *Information Sciences*, vol. 7, pp. 230–270, 1974.

[7] B. Ristic, S. Arulampalam, and N. Gordon, *Beyond the Kalman filter: Particle filters for tracking applications*. Artech House, 2004.

[8] S. C. Kramer and H. W. Sorenson, "Recursive Bayesian estimation using piece-wise constant approximations," *Automatica*, vol. 24, no. 6, pp. 789–801, 1988.

[9] A. Doucet, N. De Freitas, and N. Gordon, *Sequential Monte Carlo Methods in Practice*. Springer, 2001, ch. An Introduction to Sequential Monte Carlo Methods.

[10] K. Ito and K. Xiong, "Gaussian filters for nonlinear filtering problems," *IEEE Trans. on Automatic Control*, vol. 45, no. 5, pp. 910–927, 2000.

[11] I. Arasaratnam and S. Haykin, "Cubature Kalman filters," *IEEE Transactions on Automatic Control*, vol. 54, no. 6, pp. 1254–1269, 2009.

[12] I. Arasaratnam, S. Haykin, and R. J. Elliott, "Discrete-time nonlinear filtering algorithms using Gauss–Hermite quadrature," *Proceedings of the IEEE*, vol. 95, no. 5, pp. 953–977, 2007.

[13] S. Bhaumik *et al.*, "Cubature quadrature Kalman filter," *IET Signal Processing*, vol. 7, no. 7, pp. 533–541, 2013.

[14] B. Jia, M. Xin, and Y. Cheng, "Sparse-grid quadrature nonlinear filtering," *Automatica*, vol. 48, no. 2, pp. 327 – 341, 2012.

[15] J. Steinbring and U. D. Hanebeck, "LRKF revisited: The smart sampling Kalman filter (S^2KF)," *Journal of Advances in Information Fusion*, vol. 9, no. 2, pp. 106–123, 2014.

[16] J. Duník, O. Straka, and M. Šimandl, "Stochastic integration filter," *IEEE Transactions on Automatic Control*, vol. 58, no. 6, pp. 1561–1566, 2013.

[17] A. Genz and J. Monahan, "Stochastic integration rules for infinite regions," *SIAM Journal on Scientific Computing*, vol. 19, no. 2, pp. 426–439, 1998.

[18] A. Genz, "Methods for generating random orthogonal matrices," *Monte Carlo and Quasi-Monte Carlo Methods*, pp. 199–213, 1998.

[19] O. Straka, J. Duník, and M. Šimandl, "Unscented Kalman filter with advanced adaptation of scaling parameter," *Automatica*, vol. 50, no. 10, pp. 2657–2664, 2014.

[20] S. J. Julier and J. K. Uhlmann, "A general method for approximating nonlinear transformations of probability destributions," Dept. of Engineering Science, University of Oxford, Tech. rep., 1996.

[21] J. Pruher and O. Straka, "Gaussian process quadrature moment transform," *IEEE Transactions on Automatic Control*, vol. PP, no. 99, 2017.

[22] R. S. Bucy and K. D. Senne, "Digital synthesis of non-linear filters," *Automatica*, vol. 7, pp. 287–298, 1971.